Contribution from the Department of Chemistry and Molecular Structure Center, Indiana University, Bloomington, Indiana 47405, and School of Chemical Sciences, University of Illinois, Urbana, Illinois 61801

# Preparation, Structure, and Magnetochemistry of Hexanuclear Manganese Oxide Complexes: Chemically and Thermally Induced Aggregation of $Mn_3O(O_2CPh)_6(py)_2(H_2O)$ Forming Products Containing the $[Mn_6O_2]^{10+}$ Core

Ann R. Schake,[1a] John B. Vincent,[1a] Qiaoying Li,[1c] Peter D. W. Boyd,[1c,d] Kirsten Folting,[1b] John C. Huffman,[1b] David N. Hendrickson,*[,1c] and George Christou*[,†,1a]

*Received October 14, 1988*

A variety of synthetic procedures are described that convert the trinuclear complex $Mn_3O(O_2CPh)_6(py)_2(H_2O)$ (**1**) into the hexanuclear complexes $[Mn_6O_2(O_2CPh)_{10}(py)_2(MeCN)_2]\cdot 2MeCN$ (**2**) and $[Mn_6O_2(O_2CPh)_{10}(py)_4]\cdot Et_2O$ (**3**). With two exceptions, the procedures involve treatment of **1** with phenolic molecules (phenol, *p*-cresol, tyrosine, 2,2′-biphenol, 8-hydroxyquinoline) or the mononuclear $Mn^{III}$ complexes $[Mn(biphen)_2(biphenH)]^{2-}$ and $[Mn(Br_4biphen)_2(O_2CPh)]^{2-}$ in MeCN and lead to high (50–75%) yields of complex **2**. It is proposed that the mechanism involves reduction of the $[Mn_3O]^{6+}$ unit of **1** to a $[Mn_3O]^{5+}$ species, which spontaneously aggregates to **2** containing the $[Mn_6O_2]^{10+}$ core. This proposal is supported by the formation of **2** when **1** is reduced with the outer-sphere reductant sodium acenaphthylenide. Complex **3** is obtained in 34% yield when a PhCN solution of **1** is refluxed for 10 min. Complex **2** crystallizes in triclinic space group $P\bar{1}$ with, at −140 °C, $a$ = 15.389 (4) Å, $b$ = 19.513 (6) Å, $c$ = 14.433 (4) Å, $\alpha$ = 91.84 (1)°, $\beta$ = 94.08 (1)°, $\gamma$ = 87.85 (1)°, and $Z$ = 2. The structure was solved and refined by using 5999 unique reflections with $F > 3.0\sigma(F)$. Complex **3** crystallizes in triclinic space group $P\bar{1}$ with, at −160 °C, $a$ = 24.394 (16) Å, $\beta$ = 19.876 (11) Å, $c$ = 19.245 (12) Å, $\alpha$ = 89.71 (3)°, $\beta$ = 105.43 (3)°, $\gamma$ = 79.89 (3)°, and $Z$ = 2. The structure was solved and refined by using 6000 unique reflections with $F > 3.0\sigma(F)$. Final values of discrepancy indices $R$ ($R_w$) for **2** and **3** are 7.82 (7.17) and 7.51% (7.63%), respectively. Complex **2** contains a $[Mn_6O_2]^{10+}$ core that can be conveniently described as two edge-sharing $Mn_4$ tetrahedra at the center of each of which is a $\mu_4$-$O^{2-}$ ion. Peripheral ligation to the octahedrally coordinated Mn centers is provided by ten bridging benzoate, two terminal py, and two terminal MeCN groups. The complex is mixed valence ($Mn^{II}_4Mn^{III}_2$), and the $Mn^{III}$ centers are assigned as the two central metal ions bridged by two $O^{2-}$ ions. Complex **3** contains two independent $[Mn_6O_2]^{10+}$ complexes in the asymmetric unit, each of which is essentially identical with that in complex **2**, except that the terminal ligands are all py. The results of solid-state magnetic susceptibility studies on complex **2** in the temperature range 2.95–300 K are described. With use of the idealized symmetry of two edge-sharing tetrahedra ($D_{2h}$), the derivation by the Kambe vector-coupling method of a theoretical model to account for the intramolecular exchange interactions is described. Least-squares fitting of the susceptibility versus temperature data to the model yields the parameters $J_1$ = −42.0 $cm^{-1}$, $J_2$ = −0.8 $cm^{-1}$, $J_3$ = −2.4 $cm^{-1}$, and $g$ = 1.90, where the $J$ values refer to the $Mn^{III}$–$Mn^{III}$, $Mn^{II}$–$Mn^{III}$, and $Mn^{II}$–$Mn^{II}$ interactions, respectively. These exchange parameters give an $S_T$ = 0 ground state with two degenerate $S_T$ = 1 states at 4 $cm^{-1}$ and degenerate $S_T$ = 0, 1, 2 states at 9 $cm^{-1}$ higher in energy. The magnitudes and signs of the exchange parameters are compared with those reported for other oxo-bridged Mn complexes. Complexes **2** and **3** join a small but growing number of high-nuclearity Mn aggregates, and the prospective and potential procedures that could be employed for the synthesis of higher nuclearity Mn aggregates that might display molecular ferromagnetism are discussed.

There is considerable interest in the synthesis and study of high-nuclearity (≥4) oxide-bridged Mn complexes. This is due to a variety of reasons, not least of which is the possibility of a tetranuclear Mn unit at the water oxidation site of photosynthesis, a multidisciplinary area of study currently involving biochemical, biophysical, and inorganic chemistry researchers.[2] A better understanding of the magnetochemistry and EPR properties of high-nuclearity Mn complexes to aid in the interpretation of the often complicated data being accumulated on the native water oxidation site makes the availability of well-characterized, synthetic species invaluable. In addition, there is growing attention being focused on the preparation of models of the Fe storage protein ferritin,[3] and parallel studies with Mn are nicely complementing those in the Fe area that have led to the isolation of various high-nuclearity products.[4] These two parallel areas can provide illuminating contrasts and comparisons, not only of structural preferences between the two metals but of their electronic properties and the magnitude of the magnetic exchange interactions.

In many cases, pairwise magnetic exchange interactions between $\mu$-oxo-bridged Mn ions are ferromagnetic; thus, high-nuclearity $Mn_xO_y$ units may be attractive building blocks for molecular ferromagnets. There is a growing interest in preparing molecular ferromagnets, with some success being realized with ferromagnets comprised of organic,[5] organometallic,[6] and coordination chemistry[7] building blocks. Furthermore, fundamental information about single-domain, magnetic oxides could also be forthcoming from the characterization of discrete high-nuclearity oxide-bridged metal complexes. Single-domain particles of magnetite, $Fe_3O_4$, behave as paramagnets when their diameters are less than ~20 Å[8] and as superparamagnets in the range ~20–300 Å. In paramagnets, the magnetic moments of the metal ions act inde-

† Alfred P. Sloan Research Fellow, 1987–89; Camille and Henry Dreyfus Teacher-Scholar, 1987–92.

(1) (a) Indiana University Chemistry Department. (b) Indiana University Molecular Structure Center. (c) University of Illinois. (d) On leave from the University of Auckland, Auckland, New Zealand.
(2) (a) Dismukes, G. C. *Photochem. Photobiol.* **1986**, *43*, 99. (b) Govindjee; Kambara, T. *Proc. Natl. Acad. Sci. U.S.A.* **1985**, *82*, 6119. (c) Livorness, J.; Smith, T. D. *Struct. Bonding (Berlin)* **1982**, *48*, 2. (d) Renger, G. *Angew. Chem., Int. Ed. Engl.* **1987**, *26*, 643. (e) Christou, G.; Vincent, J. B. In *Metal Atoms in Proteins*; Que, L., Ed.; ACS Symposium Series 372; American Chemical Society: Washington, DC, 1988; Chapter 12.
(3) (a) Ford, G. C.; Harrison, P. M.; Rice, D. W.; Smith, J. M. A.; Treffry, A.; White, J. L.; Yariv, J. *Philos. Trans. R. Soc. London B* **1984**, *304*, 551. (b) Theil, E. C. *Adv. Inorg. Biochem.* **1983**, *5*, 1.
(4) (a) Wieghardt, K.; Pohl, K.; Jibril, I.; Huttner, G. *Angew. Chem., Int. Ed. Engl.* **1984**, *23*, 77. (b) Gorun, S. M.; Papaefthymiou, G. C.; Frankel, R. B.; Lippard, S. J. *J. Am. Chem. Soc.* **1987**, *109*, 3337. (c) Gerbeleu, N. V.; Batsanov, A. S.; Timko, G. A.; Struchkov, Yu. T.; Indrichan, K. M.; Popovich, G. A. *Dokl. Akad. Nauk. SSSR* **1987**, *293*, 364. (d) Armstrong, W. H.; Roth, M. E.; Lippard, S. J. *J. Am. Chem. Soc.* **1987**, *109*, 6318. (e) Gorun, S. M.; Lippard, S. J. *Inorg. Chem.* **1988**, *27*, 149.
(5) (a) McConnell, H. M. *J. Chem. Phys.* **1963**, *39*, 1910. (b) Mataga, N. *Theor. Chim. Acta* **1968**, *10*, 372. (c) Misurkin, I. A.; Ovchinnikov, A. A. *Russ. Chem. Rev. (Engl. Transl.)* **1977**, *46*, 967. (d) Breslow, R. *Pure Appl. Chem.* **1982**, *54*, 927. (e) Buchachenko, A. L. *Dokl. Akad. Nauk. SSSR* **1979**, *244*, 1146. (f) Korshak, Yu. V.; Medvedeva, T. V.; Ovchinnikov, A. A.; Spector, V. N. *Nature (London)* **1987**, *326*, 370.
(6) (a) Miller, J. S.; Epstein, A. J.; Reiff, W. M. *Acc. Chem. Res.* **1988**, *21*, 114. (b) Miller, J. S.; Epstein, A. J.; Reiff, W. M. *Chem. Rev.* **1988**, *88*, 201. (c) Miller, J. S.; Epstein, A. J.; Reiff, W. M. *NATO ASI Ser.*, in press.
(7) (a) Pei, Y.; Verdaguer, M.; Kahn, O.; Sletten, J.; Renard, J. P. *J. Am. Chem. Soc.* **1986**, *108*, 7428; *Inorg. Chem.* **1987**, *26*, 138; *J. Am. Chem. Soc.*, in press.
(8) Bate, G. In *Magnetic Oxides*; Craik, D. J., Ed.; Wiley-Interscience: New York, 1975; Part 2, Chapter 12.

0020-1669/89/1328-1915$01.50/0 

pendently of each other. In a superparamagnet, all of the individual magnetic moments in a single-domain particle are aligned parallel (or antiparallel) as a result of the interion magnetic exchange interactions. Furthermore, the net magnetization of a superparamagnet is rapidly changing direction as a result of thermal fluctuations. Magnetite particles with diameters larger than ~300–400 Å have a greater magnetic exchange interaction and, as a result, hysteresis and permanent magnetization. These phenomena have only been studied with distributions of particle sizes. Access to a series of well-characterized, higher nuclearity, oxide-bridged metal complexes could thus lead to a better understanding of the paramagnet/superparamagnet/ferromagnet interfaces.

Earlier work had established that trinuclear complexes[12a] of general formulation $[Mn_3O(O_2CR)_6L_3]^{0,+}$ (R = Me, Ph; L = py, HIm, $H_2O$) represent excellent starting points to higher nuclearity products. Thus, reaction with 2,2′-bipyridine (bpy) or salicyclic acid ($salH_2$) leads, respectively, to the tetranuclear[9,10] complexes $[Mn_4O_2(O_2CR)_{6,7}(bpy)_2]^{0,+}$ and the nonanuclear[11] complex $Mn_9O_4(O_2CPh)_8(sal)_4(salH)_2(py)_4$. To extend such reactions and establish their scope, studies have been initiated to investigate the reactivity chemistry of the trinuclear complexes in more detail. We have now determined that the $[Mn_3O]^{6+}$ core of $Mn_3O(O_2CPh)_6(py)_2(H_2O)$ (**1**) can, by a variety of procedures, be dimerized to yield $[Mn_6O_2]^{10+}$-containing products. Herein are described the syntheses, structures, and magnetochemistry of these materials.

## Experimental Section

**Compound Preparation.** The complex $Mn_3O(O_2CPh)_6(py)_2(H_2O)$ (**1**) was available from our previous work,[12b] as were the mononuclear species $(Et_3NH)_2[Mn(biphen)_2(biphenH)]$ and $(Et_3NH)_2[Mn(Br_4biphen)_2(O_2CPh)]$.[13] A solution of sodium acenaphthylenide (NaACN) was prepared by dissolving metallic sodium in a THF solution of acenaphthylene under $N_2$. Aliquots were withdrawn by syringe for use. Except where noted otherwise, all manipulations were performed under aerobic conditions. Organic reagents were used as received except acenaphthylene, which was recrystallized from warm MeOH; 2,2′-biphenol ($biphenH_2$) was available commercially whereas the tetrabromo derivative ($Br_4biphenH_2$) was prepared as described.[14]

**$[Mn_6O_2(O_2CPh)_{10}(py)_2(MeCN)_2]\cdot 2MeCN$ (2). Method A.** To a brown solution of $Mn_3O(O_2CPh)_6(py)_2(H_2O)$ (0.54 g, 0.50 mmol) in MeCN (40 mL) was added solid $(Et_3NH)_2[Mn(biphen)_2(biphenH)]$ (0.41 g, 0.50 mmol). The solid soon dissolved on stirring to give a dark orange-brown solution, which was left undisturbed at ambient temperature for several days. The resulting dark orange-brown crystals were collected by filtration, washed with MeCN, and dried under vacuum. An analogous procedure employing $(Et_3NH)_2[Mn(Br_4biphen)_2(O_2CPh)]$ (0.69 g, 0.50 mmol) yielded identical results. Yields of dried solid were in the 50–75% range. The crystallographic sample was kept in contact with the mother liquor to prevent solvent loss problems noticed in dried crystals that did not diffract. The crystallographic studies confirmed the title formulation, but dried samples analyzed for $Mn_6O_2(O_2CPh)_{10}(py)_2(MeCN)_2(H_2O)_2$, suggesting MeCN loss and absorption of $H_2O$ molecules; the latter was supported by the observed $H_2O$ peaks in the infrared spectrum. Anal. Calcd for $C_{84}H_{70}N_4O_{24}Mn_6$: C, 54.56; H, 3.82; N, 3.03; Mn, 17.83. Found: C, 53.9; H, 3.7; N, 2.65; Mn, 18.1. Electronic spectrum [EtCN; $\lambda_{max}$, nm ($\epsilon_M/Mn_6$, L mol$^{-1}$ cm$^{-1}$)]: 490 (1010). IR data (Nujol): 3400 (s, br), 2275 (w), 1605 (s), 1565 (s), 1540 (s), 1215 (w), 1180 (m), 1150 (w), 1065 (m), 1030 (w), 1020 (m), 1005 (w), 930 (w), 840 (m), 830 (m), 820 (m), 750 (w), 720 (s), 700 (m), 685 (m), 670 (s), 610 (s), 560 (m), 470 (m), 420 (m), 400 cm$^{-1}$ (m).

**Table I.** Crystallographic Data for Complexes **2** and **3**

| param | **2** | **3** |
|---|---|---|
| formula | $C_{88}H_{72}N_6O_{22}Mn_6$ | $C_{184}H_{150}N_8O_{45}Mn_{12}$ |
| space group | $P\bar{1}$ | $P\bar{1}$ |
| temp, °C | −140 | −160 |
| $a$, Å | 15.389 (4)[a] | 24.394 (16)[b] |
| $b$, Å | 19.513 (6) | 19.876 (11) |
| $c$, Å | 14.433 (4) | 19.245 (12) |
| $\alpha$, deg | 91.84 (1) | 89.71 (3) |
| $\beta$, deg | 94.08 (1) | 105.43 (3) |
| $\gamma$, deg | 87.85 (1) | 79.89 (3) |
| $Z$ | 2 | 2 |
| V, Å$^3$ | 4318.10 | 8841.63 |
| radiation (λ, Å) | Mo Kα (0.71069[c]) | Mo Kα (0.71069[c]) |
| abs coeff, cm$^{-1}$ | 8.877 | 8.698 |
| scan speed, deg min$^{-1}$ | 4.0 | 10.0 |
| $\rho_{calc}$, g cm$^{-3}$ | 1.436 | 1.477 |
| tot. no. of data | 12611 | 24327 |
| no. of unique data | 11349 | 23225 |
| averaging $R$ | 0.059[d] | 0.108[e] |
| no. of obsd data ($F > 3\sigma(F)$) | 5999 | 6000 |
| $R$ ($R_w$), % | 7.82 (7.17) | 7.51 (7.63) |
| goodness of fit | 1.293 | 2.072 |

[a] Reflections (38) at −140 °C. [b] Reflections (30) at −160 °C. [c] Graphite monochromator. [d] Reflections (1262) measured more than once. [e] Reflections (1102) measured more than once.

The solid is soluble without degradation only in EtCN and PhCN.

**Method B.** To a brown solution of $Mn_3O(O_2CPh)_6(py)_2(H_2O)$ (0.54 g, 0.5 mmol) in MeCN (15 mL) was added phenol (0.60 g, 6.4 mmol) with stirring. The solid soon dissolved to give a dark orange-brown solution, followed by the appearance of orange-brown crystals. When precipitation was judged to be complete, the crystals were filtered, washed with MeCN, and dried under vacuum. Analogous procedures employing the phenolic molecules biphenol, *p*-cresol, tyrosine, and 8-hydroxyquinoline (0.5 mmol) gave identical results. Yields were ~60%. The dried product from the phenol reaction analyzed as $Mn_6O_2(O_2CPh)_{10}(py)(MeCN)_{1.5}(H_2O)_3$. Anal. Calcd for $C_{78}H_{65.5}N_{2.5}O_{25}Mn_6$: C, 53.00; H, 3.74; N, 1.98; Mn, 18.65. Found: C, 52.9; H, 3.6; N, 1.8; Mn, 18.65. The IR spectra were all essentially identical with that detailed under method A.

**Method C.** To a brown solution of $Mn_3O(O_2CPh)_6(py)_2(H_2O)$ (0.54 g, 0.50 mmol) in MeCN (40 mL) was added a THF solution of NaACN (0.5 M, 1.0 mL, 0.5 mmol) under nitrogen. Anaerobic conditions were then discontinued, and the orange-brown solution was left undisturbed at ambient temperature for several days until precipitation of orange-brown crystals was judged complete. The product was collected by filtration, washed with MeCN, and dried under vacuum. The yield was 50%, and the IR spectrum corresponded to that detailed above. Anal. Calcd for $C_{84}H_{68}N_4O_{23}Mn_6$: C, 55.10; H, 3.74; N, 3.06; Mn, 18.00. Found: C, 54.7; H, 3.0; N, 2.9; Mn, 18.1.

**$[Mn_6O_2(O_2CPh)_{10}(py)_4]\cdot Et_2O$ (3).** A brown solution of $Mn_3O(O_2CPh)_6(py)_2(H_2O)$ (3.0 g, 2.77 mmol) in PhCN (15 mL) was heated and maintained at reflux (188 °C) for 10 min. The resulting red-brown solution was cooled and layered with a mixture of hexanes (25 mL) and $Et_2O$ (10 mL). After several days, large red-brown crystals were collected by filtration, washed with hexanes, and dried in air; the yield was 34%. Anal. Calcd for $C_{94}H_{80}N_4O_{23}Mn_6$: C, 57.51; H, 4.11; N, 2.85; Mn, 16.79. Found: C, 57.7; H, 3.8; N, 3.1; Mn, 17.3.

**X-ray Crystallography and Structure Solution.** Data were collected on a Picker four-circle diffractometer using standard low-temperature facilities; details of the diffractometry, low-temperature facilities, and computational procedures employed by the Molecular Structure Center are available elsewhere.[15] Data collection parameters are summarized in Table I. The structures were solved by a combination of direct-methods (MULTAN) and Fourier techniques and refined by full-matrix least squares.

For both complexes **2** and **3**, a systematic search of a limited hemisphere of reciprocal space yielded a set of reflections that exhibited no symmetry or systematic extinctions. The choice of the centrosymmetric triclinic space group $P\bar{1}$ was confirmed by the successful solution and refinement of the structures. For **2**, the intensities of four standard reflections measured every 300 reflections remained constant within experimental error throughout the data collection. Following usual data

(9) (a) Vincent, J. B.; Christmas, C.; Huffman, J. C.; Christou, G.; Chang, H.-R.; Hendrickson, D. N. *J. Chem. Soc., Chem. Commun.* **1987**, 236. (b) Christmas, C.; Vincent, J. B.; Huffman, J. C.; Christou, G.; Chang, H.-R.; Hendrickson, D. N. *J. Chem. Soc., Chem. Commun.* **1987**, 1303.
(10) Vincent, J. B.; Christmas, C.; Chang, H.-R.; Li, Q.; Boyd, P. D. W.; Huffman, J. C.; Hendrickson, D. N.; Christou, G. *J. Am. Chem. Soc.* **1989**, *111*, 2086.
(11) Christmas, C.; Vincent, J. B.; Chang, H.-R.; Huffman, J. C.; Christou, G.; Hendrickson, D. N. *J. Am. Chem. Soc.* **1988**, *110*, 823.
(12) (a) For a review of trinuclear "basic carboxylates", see: Catterick, J.; Thornton, P. *Adv. Inorg. Chem. Radiochem.* **1977**, *20*, 291. (b) Vincent, J. B.; Chang, H.-R.; Folting, K.; Huffman, J. C.; Christou, G.; Hendrickson, D. N. *J. Am. Chem. Soc.* **1987**, *109*, 5703.
(13) Schake, A. R.; Christou, G. Unpublished work.
(14) Diels, O.; Bibergeil, A. *Ber. Dtsch. Chem. Ges.* **1902**, *35*, 306.
(15) Chisholm, M. H.; Folting, K.; Huffman, J. C.; Kirkpatrick, C. C. *Inorg. Chem.* **1984**, *23*, 1021.

processing and averaging of equivalent reflections, a unique set of 11 349 reflections was obtained, of which 5999 were considered observed ($F > 3.00\sigma(F)$). The non-hydrogen atoms were readily located, including those of two MeCN solvate molecules. Due to the large number of independent atoms, only the Mn atoms were refined with anisotropic thermal parameters, the other non-hydrogen atoms being refined isotropically. In the final refinement cycles, the hydrogen atoms of the aromatic rings were included in fixed, calculated positions. The final values of $R$ and $R_w$ are included in Table I. The final difference map was essentially featureless, the largest peak being 0.65 e/Å$^3$.

For complex **3**, data were collected at 10°/min due to the large unit cell and expected number of reflections. Near the middle of the data collection the crystal fragmented into two, and one piece was lost. The remaining fragment still diffracted well and, due to the time already invested, the decision was made to complete data collection and scale the two sets of data by using the 3 standard reflections measured every 400 reflections (whose intensities did not change with time). After scaling, usual data processing, and averaging of equivalent reflections, a set of 23 225 reflections remained of which only 6000 ($F > 3.0\sigma(F)$) were employed for structure solution. The non-hydrogen atoms were readily located, and the asymmetric unit was found to consist of two independent $Mn_6$ units, labeled with the suffixes A and B in Table III and the supplementary material. The ether molecule was also located in the lattice, but well separated from the $Mn_6$ molecules. Due to the large number of independent atoms only the Mn atoms were refined with anisotropic thermal parameters, the remaining non-hydrogen atoms being refined isotropically. No attempt to include hydrogen atoms was made. Some disorder problems were noticed with some of the aromatic rings, but no attempt to correct for these was made due to program limitations arising from the number of independent atoms (249). The final difference map showed only a few peaks, well separated from the $Mn_6$ molecules, which were indicative of disordered additional solvate molecules, but these were not included. Final values of $R$ and $R_w$ are listed in Table I.

**Physical Measurements.** Variable-temperature magnetic susceptibility data were measured by using a Series 800 VTS-50 SQUID susceptometer (SHE Corp.) maintained by the Physics Department of the University of Illinois. The susceptometer was operated at a magnetic field strength of 10 kG. Diamagnetic corrections were estimated from Pascal's constants and subtracted from the experimental susceptibility of the compound. The molar susceptibility vs temperature data were fit to the appropriate theoretical expression by means of a least-squares-fitting computer program.[16]

## Results and Discussion

**Syntheses.** To minimize the parameters involved, the mixed-valence (II,III,III) trinuclear complex $Mn_3O(O_2CPh)_6(py)_2(H_2O)$ (**1**) was employed throughout this work. A total of nine reactions have now been found that convert this material to $Mn_6O_2(O_2CPh)_{10}L_4$ (L = py, MeCN), and these are detailed as four separate procedures in the Experimental Section. Initial success was obtained in reactions with $[Mn(biphen)_2(biphenH)]^{2-}$, $[Mn(Br_4biphen)_2(O_2CPh)]^{2-}$, and the phenolic molecules phenol, *p*-cresol, tyrosine, and 8-hydroxyquinoline in MeCN. In each case, good yields (50–75%) of pure, orange-brown material were obtained by employing facile one-step reactions. The well-formed crystals were found to undergo solvent loss on drying; the crystallographic studies were therefore performed on a sample maintained in contact with the mother liquor, and the formulation $[Mn_6O_2(O_2CPh)_{10}(py)_2(MeCN)_2]\cdot 2MeCN$ (**2**) was established (vide infra). On drying under vacuum, however, not only did the crystals lose bound and lattice solvent but the resulting solid appeared hygroscopic, as evidenced by the presence of strong $H_2O$ bands in the IR spectra. Analytical data supported this, consistently indicating a formulation $Mn_6O_2(O_2CPh)_{10}(py)_x(MeCN)_y(H_2O)_z$.

The formula of the hexanuclear complex establishes it as being mixed valence ($Mn^{II}_4Mn^{III}_2$). Without any mechanistic implication, we suggest the overall aggregation is triggered by reduction of the $[Mn_3O]^{6+}$ unit ($Mn^{II}Mn^{III}_2$) to $[Mn_3O]^{5+}$ ($Mn^{II}_2Mn^{III}$) with concomitant oxidation of the phenolic reagent. Trinuclear species at this oxidation level, viz. $[Mn_3O(O_2CR)_6L_3]^-$, are unknown in inorganic chemistry, and it seems reasonable to conclude that they are unstable with respect to aggregation, as summarized in eq 1.

$$[Mn_3O]^{6+} + e^- \rightarrow [Mn_3O]^{5+} \rightarrow \tfrac{1}{2}[Mn_6O_2]^{10+} \quad (1)$$

The ability of $Mn^{III}$ to oxidize phenolic substrates is well-known, and the use of $Mn^{III}$ complexes (including $Mn_3O$-containing materials) for such oxidations is common in organic chemistry.[17] Also, the $[Mn_6O_2]$ core is structurally akin to two fused $[Mn_3O]$ units (vide infra). The reactions with the mononuclear $Mn^{III}$ reagents must be more complicated due to the presence of additional metal ions but, overall, essentially the same chemistry is probably involved.

Since the phenolic reagents employed are good metal-binding ligands, in addition to being oxidizable, it seemed possible that formation of the $Mn_6$ product could be proceeding by prior attachment of the phenolic group to the $Mn_3$ complex (perhaps by carboxylate displacement) followed by inner-sphere electron transfer from ligand to Mn. Whether such a prior binding step is mechanistically essential or merely coincidental to the core dimerization was explored by employing a reducing agent that may be reasonably assumed to be operating by an outer-sphere electron-transfer mechanism. The reductant chosen was the organic radical anion acenaphthylenide ($ACN^-$). Treatment of a solution of complex **1** in MeCN with 1 equiv of NaACN generated an orange-brown solution from which complex **2** crystallizes on standing in ~50% yield. This result supports both eq 1 and reduction of the trinuclear unit as the sole essential step that triggers aggregation to **2**. This mechanistically simpler reductive dimerization can be summarized in eq 2.

$$2Mn_3O(O_2CPh)_6(py)_2(H_2O) + 2NaACN \xrightarrow{MeCN} Mn_6O_2(O_2CPh)_{10}(py)_2(MeCN)_2 + 2NaO_2CPh + 2py + 2ACN + H_2O \quad (2)$$

An additional procedure has been found for converting **1** into a hexanuclear product, i.e. high temperatures. A PhCN solution of **1** was heated and maintained at reflux for ca. 10 min; from the cooled solution was isolated $[Mn_6O_2(O_2CPh)_{10}(py)_4]\cdot Et_2O$ (**3**). Data were collected and the structure was solved because the unit cell dimensions were much larger than those for **2** and it was originally believed that a higher (>6) nuclearity product had been obtained; instead, the structure solution showed two independent $Mn_6O_2$ species per asymmetric unit. The source of electrons in this conversion is unclear, but under these high thermal conditions oxidation of solvent, its impurities, and/or ligands could be occurring. Prolonged reflux leads to lowered yields of **3**, presumably due to thermal decomposition. It is interesting that **3** contains four py groups rather than two as in **2**; presumably this is due to the poorer coordinating ability of PhCN vs MeCN, inhibiting replacement of py. Note also that the two brief communications of complexes containing $[Mn_6O_2]$ cores also employed high-thermal conditions: $Mn_6O_2(piv)_{10}(pivH)_4$ (pivH = pivalic acid) was obtained by refluxing a toluene solution of $MnCO_3$ and pivalic acid[18] and, more recently,[19] by refluxing a dioxane solution of $Mn(NO_3)_2$ and pivalic acid. In both cases the absence of a coordinating solvent led to the four terminal positions being occupied by pivalic acid molecules.

**Description of Structures.** The molecular structures of complexes **2** and **3** are depicted in Figures 1 and 2, respectively. Approximately equivalent views are presented for easy comparison. The labeling schemes are similar but not identical. Fractional coordinates and selected bond lengths and angles for **2** are given in full detail in Tables II and IV, respectively. Because the structure of **3** is essentially identical with that of **2** except for terminal ligation, and since the two independent molecules of **3** are almost identical within the $3\sigma$ criterion, we have relegated full listing of the fractional coordinates and bond lengths and angles of **3** to the supplementary material; in Tables III and V, therefore, are listed these parameters for only the $[Mn_6O_2]$ cores, facilitating comparison with **2**.

(16) Chandler, J. P. *QCPE* **1973**, 66.

(17) Arndt, D. *Manganese Compounds as Oxidizing Agents in Organic Chemistry*; Open Court: La Salle, IL, 1981.

(18) Baikie, A. R. E.; Howes, A. J.; Hursthouse, M. B.; Quick, A. B.; Thornton, P. *J. Chem. Soc., Chem. Commun.* **1986**, 1587.

(19) Gerbeleu, N. V.; Batsanov, A. S.; Timko, G. A.; Struchkov, Yu. T.; Indrichan, K. M.; Popovich, G. A. *Dokl. Akad. Nauk. SSSR* **1987**, *294*, 256.

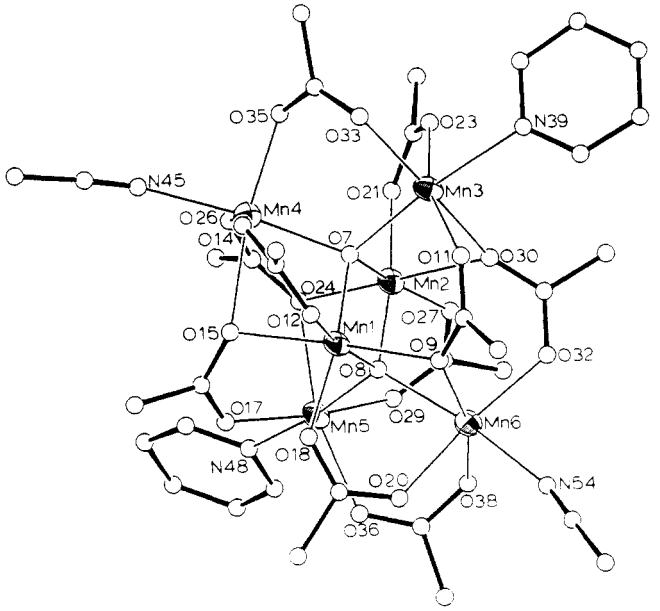


**Figure 1.** Molecular structure of $[Mn_6O_2(O_2CPh)_{10}(py)_2(MeCN)_2]\cdot 2MeCN$ (**2**). To avoid congestion, only one of the phenyl carbon atoms of each benzoate ligand is shown. Carbon atoms are numbered consecutively around aromatic rings and along MeCN groups. The numbering of carboxylate carbon atoms is intermediate between those of its bound oxygen atoms.

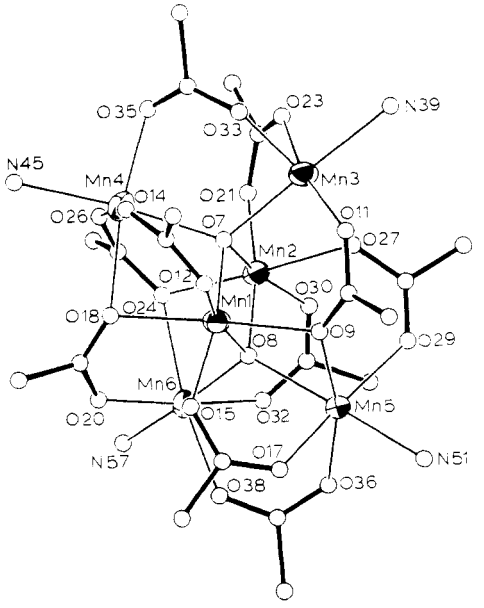


**Figure 2.** Molecular structure of $[Mn_6O_2(O_2CPh)_{10}(py)_4]\cdot Et_2O$ (**3**). To avoid congestion, pyridine carbon atoms are omitted and only one of the phenyl carbon atoms of each benzoate ligand is shown. The carbon numbering sequence is as for Figure 1.

The structure of **2** consists of six Mn atoms arranged as two edge-sharing tetrahedra. At the center of each tetrahedron lies a $\mu_4$-$O^{2-}$ ion. Peripheral ligation is accomplished by ten bridging benzoate, two terminal py, and two terminal MeCN groups. Each Mn is six-coordinate and possesses distorted octahedral geometry. Charge considerations indicate a mixed-valence $Mn^{II}_4Mn^{III}_2$ description, and the $Mn^{III}$ centers are assigned as central Mn(1) and Mn(2). This is based, primarily, on consideration of the structural parameters in Table IV. Thus, Mn(1,2)–O(7,8) distances (average 1.88 Å) are noticeably shorter than Mn(3,4,5,6)–O(7,8) distances (average 2.196 Å), consistent with the higher oxidation state in the former. Similarly, Mn(1,2)–carboxylate distances (average 2.096 Å) are noticeably shorter than Mn(3,4,5,6)–carboxylate distances (average 2.177 Å). The $Mn^{III}$ pair is consequently bridged by two $\mu_4$-$O^{2-}$ whereas each $Mn^{II}Mn^{III}$ and $Mn^{II}Mn^{II}$ pair is bridged by only one $\mu_4$-$O^{2-}$. The ten benzoate groups separate into two classes. Six are $\mu_2$ with each of their carboxylate oxygen atoms being terminally ligated to a Mn. The other four benzoates are $\mu_3$ with one carboxylate oxygen atom terminally ligated to a $Mn^{II}$, whereas the other carboxylate oxygen is bridging a $Mn^{II}Mn^{III}$ pair; the latter four oxygen atoms are O(9,15,24,30). This is an extremely unusual bridging mode for a carboxylate ligand, and we are unaware of a previous example, except for the corresponding pivalate complexes.[18,19] The two $Mn^{III}$ atoms also show the Jahn–Teller distortion expected for an octahedral high-spin $d^4$ ion, taking the form of an axial elongation with the $\mu_2$-oxygen atoms O(9,15,24,30) of the unusual $\mu_3$-benzoate groups occupying axial positions. Finally, each remaining terminal position at the $Mn^{II}$ sites is occupied by either a py or MeCN group. This mixed ligation is surprising given the near equivalence of the four $Mn^{II}$ centers and the absence of any observable py/MeCN disorder. Why partial rather than no or complete substitution of py by solvent MeCN has occurred is difficult to rationalize.

The $M_4(\mu_4\text{-}O^{2-})$ units comprising the core have extensive precedence in inorganic chemistry. This "beryllium acetate" structure is a commonly encountered moiety,[12a,20] but most known examples are to be found in Cu chemistry and there are no characterized examples with Mn.

In addition to the "edge-sharing tetrahedra" description of the $Mn_6O_2$ core, two alternative ways of describing it can be presented that emphasize its structural relationship to smaller nuclearity Mn/O units: (i) The $Mn_6O_2$ unit can be considered as two $[Mn_3O]^{5+}$ units, joined together by each of the $\mu_3$-$O^{2-}$ atoms becoming $\mu_4$ by ligating to the $Mn^{III}$ center of the adjacent $Mn_3O$ unit. This also relates to the synthetic procedure for making complex **2** from **1**, for reduction of the latter yields the $[Mn_3O]^{5+}$ core and it could be argued that lowering the average metal oxidation state permits the basicity of the $\mu_3$-$O^{2-}$ to increase sufficiently to allow ligation to an additional metal center. The two $[Mn^{II}_2Mn^{III}O]^{5+}$ units comprising the $Mn_6O_2$ core of **2**, and conceptually representing its parentage, are Mn(1,3,4)O(7) and Mn(2,5,6)O(8) or, alternatively, Mn(2,3,4)O(7) and Mn(1,5,6)O(8). (ii) The $Mn_6O_2$ core can be considered to contain the $[Mn^{II}_2Mn^{III}_2O_2]$ core of $Mn_4O_2(OAc)_6(bpy)_2$.[9b] The latter possesses a planar $Mn_4$ rhombus with two $\mu_3$-$O^{2-}$ bridges, one above and one below the plane. This unit is to be found within **2** (Mn(1,2,3,5)O(7,8) or Mn(1,2,4,6)O(7,8)), and completion of the $Mn_6O_2$ core then requires merely the conversion of the two $\mu_3$-$O^{2-}$ to $\mu_4$-$O^{2-}$ by ligation to an additional $Mn^{II}$ center. The "short" $Mn^{III}\cdots Mn^{III}$ (2.820 (3) Å) and "long" $Mn^{II}\cdots Mn^{III}$ (3.1–3.5 Å) distances compare favorably with those in $Mn_4O_2(OAc)_6(bpy)_2$ (2.779 (1) and 3.3–3.5 Å, respectively). Also note that, although the oxidation levels do not correspond, the $Mn_6O_2$ unit also contains the nonplanar "butterfly"-like $Mn_4O_2$ unit found in $[Mn^{III}_4O_2(OAc)_7(bpy)_2]^+$.[9a] Such a unit in **2** would be that formed by Mn(1,2,3,6)O(7,8) or Mn(1,2,4,5)O(7,8), with Mn(1,2) representing the "hinge" or "backbone" positions, and completion of $Mn_6O_2$ again requires conversion of $\mu_3$-$O^{2-}$ to $\mu_4$-$O^{2-}$ by ligation to additional Mn sites. Thus, the planar and butterfly-like $Mn_4O_2$ units represent the products from two possible ways of removing two Mn atoms from the $Mn_6O_2$ core, as shown:

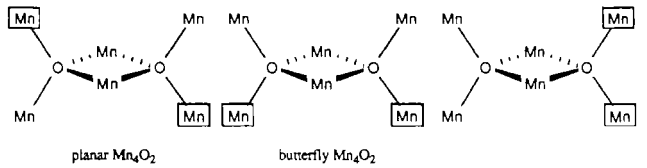


The third possibility would yield a $Mn_4(\mu_2\text{-}O)(\mu_4\text{-}O)$ unit; this is currently unknown.

The structure of complex **3** is essentially identical with that of **2** except for all terminal ligands being py. The two independent molecules of **3** are identical within $3\sigma$, and the partial listing of

(20) Guy, J. T.; Cooper, J. C.; Gilardi, R. D.; Flippen-Anderson, J. L.; George, C. F. *Inorg. Chem.* **1988**, *27*, 635.

**Table II.** Fractional Coordinates ($\times 10^4$) and Thermal Parameters ($Å^2 \times 10$) for **2**

| atom | x | y | z | $B_{iso}$ | atom | x | y | z | $B_{iso}$ |
|---|---|---|---|---|---|---|---|---|---|
| Mn(1) | 8290 (1) | 2872 (1) | 4724 (1) | 21 | C(62) | 8297 (9) | 5142 (7) | 5910 (10) | 37 (3) |
| Mn(2) | 6988 (1) | 2004 (1) | 5229 (1) | 21 | C(63)[c] | 10786 (8) | 3179 (7) | 6078 (9) | 31 (3) |
| Mn(3) | 8131 (1) | 2435 (1) | 7061 (1) | 22 | C(64) | 10769 (10) | 3885 (8) | 6068 (10) | 45 (3) |
| Mn(4) | 9165 (1) | 1415 (1) | 5176 (1) | 22 | C(65) | 11461 (12) | 4245 (9) | 6519 (12) | 62 (4) |
| Mn(5) | 6752 (1) | 2163 (1) | 3054 (1) | 24 | C(66) | 12163 (15) | 3895 (12) | 6932 (15) | 87 (6) |
| Mn(6) | 6517 (1) | 3723 (1) | 4701 (1) | 25 | C(67) | 12162 (14) | 3188 (11) | 7001 (14) | 81 (5) |
| O(7) | 8172 (5) | 2172 (4) | 5582 (5) | 22 (2) | C(68) | 11457 (10) | 2817 (8) | 6563 (11) | 49 (4) |
| O(8) | 7115 (5) | 2708 (4) | 4391 (5) | 22 (2) | C(69)[c] | 9553 (8) | 2085 (6) | 2409 (8) | 22 (2) |
| O(9) | 7800 (5) | 3780 (4) | 5563 (5) | 23 (2) | C(70) | 10366 (9) | 1865 (7) | 2752 (9) | 33 (3) |
| C(10) | 8138 (8) | 3920 (6) | 6388 (8) | 24 (2) | C(71) | 11071 (9) | 1858 (7) | 2199 (10) | 37 (3) |
| O(11) | 8338 (5) | 3500 (4) | 6989 (5) | 23 (2) | C(72) | 10941 (10) | 2089 (7) | 1303 (10) | 42 (3) |
| O(12) | 9428 (5) | 3142 (4) | 5253 (5) | 22 (2) | C(73) | 10148 (10) | 2324 (8) | 967 (10) | 44 (3) |
| C(13) | 10069 (8) | 2783 (6) | 5582 (8) | 25 (2) | C(74) | 9462 (10) | 2318 (7) | 1507 (10) | 42 (3) |
| O(14) | 10155 (5) | 2147 (4) | 5549 (5) | 27 (2) | C(75)[c] | 8117 (8) | 4144 (6) | 2346 (9) | 27 (3) |
| O(15) | 8926 (5) | 2053 (4) | 3854 (5) | 27 (2) | C(76) | 8903 (9) | 3987 (7) | 2027 (10) | 37 (3) |
| C(16) | 8776 (8) | 2083 (6) | 2975 (9) | 28 (3) | C(77) | 9115 (9) | 4241 (7) | 1165 (10) | 41 (3) |
| O(17) | 8034 (5) | 2139 (4) | 2567 (5) | 27 (2) | C(78) | 8502 (11) | 4647 (8) | 693 (11) | 50 (4) |
| O(18) | 8433 (5) | 3459 (4) | 3662 (5) | 26 (2) | C(79) | 7721 (9) | 4798 (7) | 1006 (9) | 35 (3) |
| C(19) | 7894 (8) | 3886 (6) | 3279 (8) | 26 (2) | C(80) | 7491 (8) | 4547 (7) | 1845 (9) | 32 (3) |
| O(20) | 7216 (5) | 4118 (4) | 3601 (5) | 27 (2) | C(81)[c] | 6849 (8) | 435 (6) | 7206 (8) | 25 (3) |
| O(21) | 6906 (5) | 1187 (4) | 5965 (5) | 25 (2) | C(82) | 7256 (9) | 198 (7) | 8030 (9) | 34 (3) |
| C(22) | 7116 (8) | 1075 (6) | 6826 (8) | 24 (2) | C(83) | 7033 (9) | −415 (7) | 8374 (10) | 39 (3) |
| O(23) | 7566 (5) | 1479 (4) | 7342 (5) | 27 (2) | C(84) | 6392 (10) | −789 (7) | 7911 (10) | 42 (3) |
| O(24) | 7143 (5) | 1277 (4) | 4026 (5) | 24 (2) | C(85) | 5981 (10) | −570 (8) | 7113 (10) | 43 (3) |
| C(25) | 7617 (8) | 740 (6) | 4050 (8) | 23 (2) | C(86) | 6211 (9) | 44 (7) | 6743 (9) | 33 (3) |
| O(26) | 8351 (5) | 679 (4) | 4485 (6) | 28 (2) | C(87)[c] | 7322 (8) | 124 (6) | 3473 (8) | 25 (3) |
| O(27) | 5725 (5) | 2000 (4) | 5024 (5) | 24 (2) | C(88) | 6427 (9) | 53 (7) | 3236 (9) | 32 (3) |
| C(28) | 5223 (8) | 1997 (6) | 4270 (8) | 25 (2) | C(89) | 6143 (9) | −502 (7) | 2678 (10) | 39 (3) |
| O(29) | 5465 (5) | 1956 (4) | 3463 (5) | 26 (2) | C(90) | 6731 (10) | −972 (8) | 2391 (10) | 43 (3) |
| O(30) | 6708 (5) | 2669 (4) | 6469 (5) | 21 (2) | C(91) | 7609 (9) | −931 (7) | 2610 (9) | 35 (3) |
| C(31) | 6056 (8) | 3085 (6) | 6501 (8) | 23 (2) | C(92) | 7907 (8) | −377 (6) | 3190 (9) | 29 (3) |
| O(32) | 5858 (5) | 3525 (4) | 5894 (6) | 28 (2) | C(93)[c] | 4279 (8) | 2059 (6) | 4398 (8) | 24 (3) |
| O(33) | 9335 (5) | 1924 (4) | 7483 (6) | 28 (2) | C(94) | 3703 (8) | 2303 (6) | 3690 (9) | 28 (3) |
| C(34) | 9518 (8) | 1307 (7) | 7283 (9) | 28 (3) | C(95) | 2813 (9) | 2354 (7) | 3817 (10) | 38 (3) |
| O(35) | 9311 (5) | 1002 (4) | 6517 (6) | 29 (2) | C(96) | 2485 (10) | 2167 (8) | 4624 (10) | 43 (3) |
| O(36) | 6129 (5) | 3048 (4) | 2420 (5) | 25 (2) | C(97) | 3056 (10) | 1906 (8) | 5312 (11) | 49 (4) |
| C(37) | 5616 (8) | 3466 (6) | 2785 (9) | 26 (2) | C(98) | 3939 (9) | 1875 (7) | 5200 (9) | 35 (3) |
| O(38) | 5512 (5) | 3522 (4) | 3655 (5) | 25 (2) | C(99)[c] | 5474 (8) | 3032 (6) | 7275 (8) | 26 (3) |
| N(39)[a] | 7805 (6) | 2698 (5) | 8560 (7) | 24 (2) | C(100) | 5559 (9) | 2463 (7) | 7829 (10) | 37 (3) |
| C(40) | 7353 (9) | 3241 (7) | 8796 (9) | 32 (3) | C(101) | 5003 (10) | 2423 (8) | 8551 (11) | 48 (4) |
| C(41) | 7025 (10) | 3339 (8) | 9666 (10) | 44 (3) | C(102) | 4402 (11) | 2942 (9) | 8720 (12) | 54 (4) |
| C(42) | 7146 (9) | 2833 (7) | 10275 (10) | 39 (3) | C(103) | 4336 (10) | 3513 (8) | 8192 (11) | 44 (3) |
| C(43) | 7610 (9) | 2248 (7) | 10032 (10) | 42 (3) | C(104) | 4878 (9) | 3552 (7) | 7447 (9) | 33 (3) |
| C(44) | 7933 (9) | 2190 (7) | 9155 (10) | 38 (3) | C(105)[c] | 9989 (8) | 857 (6) | 8003 (8) | 26 (3) |
| N(45)[b] | 10314 (7) | 792 (5) | 4695 (7) | 32 (2) | C(106) | 10090 (9) | 160 (7) | 7876 (9) | 36 (3) |
| C(46) | 10961 (9) | 618 (6) | 4447 (9) | 29 (3) | C(107) | 10521 (9) | −252 (7) | 8528 (9) | 35 (3) |
| C(47) | 11798 (9) | 424 (7) | 4082 (10) | 42 (3) | C(108) | 10867 (10) | 50 (8) | 9348 (11) | 46 (4) |
| N(48)[a] | 6423 (6) | 1473 (5) | 1776 (7) | 27 (2) | C(109) | 10788 (9) | 751 (8) | 9492 (10) | 41 (3) |
| C(49) | 5636 (8) | 1539 (6) | 1336 (9) | 29 (3) | C(110) | 10345 (10) | 1161 (8) | 8825 (10) | 44 (3) |
| C(50) | 5378 (9) | 1110 (7) | 579 (9) | 36 (3) | C(111)[c] | 5071 (8) | 3941 (6) | 2181 (9) | 28 (3) |
| C(51) | 5936 (9) | 611 (7) | 289 (10) | 40 (3) | C(112) | 4566 (9) | 4454 (7) | 2579 (10) | 38 (3) |
| C(52) | 6760 (10) | 523 (7) | 745 (10) | 42 (3) | C(113) | 4034 (11) | 4912 (9) | 2023 (12) | 58 (4) |
| C(53) | 6965 (8) | 977 (6) | 1488 (9) | 28 (3) | C(114) | 4073 (12) | 4833 (9) | 1084 (13) | 61 (4) |
| N(54)[b] | 6144 (7) | 4854 (6) | 4928 (7) | 33 (2) | C(115) | 4553 (11) | 4333 (9) | 687 (12) | 57 (4) |
| C(55) | 6138 (8) | 5424 (7) | 4944 (9) | 29 (3) | C(116) | 5069 (9) | 3873 (7) | 1223 (10) | 35 (3) |
| C(56) | 6147 (9) | 6167 (7) | 4990 (10) | 39 (3) | N(117)[d] | 6564 (12) | −2133 (10) | 9441 (13) | 90 (5) |
| C(57)[c] | 8279 (8) | 4664 (6) | 6606 (8) | 23 (2) | C(118) | 6757 (12) | −2626 (10) | 9041 (13) | 60 (4) |
| C(58) | 8473 (9) | 4881 (7) | 7533 (9) | 34 (3) | C(119) | 7102 (12) | −3206 (10) | 8650 (13) | 67 (5) |
| C(59) | 8637 (9) | 5556 (7) | 7779 (10) | 41 (3) | N(120)[d] | 8742 (12) | 6407 (9) | 214 (13) | 85 (5) |
| C(60) | 8668 (10) | 6018 (8) | 7095 (11) | 52 (4) | C(121) | 9251 (13) | 6457 (9) | 818 (13) | 62 (4) |
| C(61) | 8500 (10) | 5826 (8) | 6144 (11) | 48 (3) | C(122) | 9898 (12) | 6536 (10) | 1573 (13) | 68 (5) |

[a] Terminal pyridine. [b] Terminal MeCN. [c] Beginning of phenyl ring. [d] Solvate MeCN.

structural parameters in Table V shows the near congruency of the $Mn_6O_2$ cores of complexes **2** and **3**. Thus, the identity of the terminal ligands has little influence on the cores. Note, incidentally, that in neither **2** nor **3** does the $Mn_6O_2$ core possess the idealized $D_{2h}$ symmetry of two edge-sharing tetrahedra, as is most apparent from the various bond lengths and angles listed in Tables III and V. However, in both complexes the pattern of distortion away from $D_{2h}$ is similar and therefore cannot be a consequence of the ligand asymmetry in **2**.

**Magnetic Susceptibility of $[Mn_6O_2(O_2CPh)_{10}(py)_2(MeCN)_2]\cdot 2MeCN$.** The variable-temperature magnetic susceptibility of $[Mn_6O_2(O_2CPh)_{10}(py)_2(MeCN)_2]\cdot 2H_2O$ (**2**)[21a] was measured in the range 2.95–300 K. The effective magnetic moment per $Mn_6$ cluster falls from 11.57 $\mu_B$ at 399 K to 2.46 $\mu_B$ at 2.95 K (Figure 3), the rate of decrease increasing below 50 K. The molar paramagnetic susceptibility increases with decreasing temperature, reaching a maximum at ~13 K and then decreasing slightly (Figure 4).

An examination of the structure of **2** shows two central bis($\mu$-oxide)-bridged $Mn^{III}$ ($S = 2$) ions bridged to four $Mn^{II}$ ($S = {}^5/_2$) ions via single $\mu$-oxide bridges (Figure 1). The bridging

(21) (a) The sample employed was the analytical sample from method A. (b) Kambe, K. *J. Phys. Soc. Jpn.* **1950**, *5*, 48.

**Table III.** Fractional Coordinates (×10⁴) and Thermal Parameters (Å² × 10) for **3**

| atom[a] | x | y | z | $B_{iso}$ |
|---|---|---|---|---|
| Mn(1)A | 3199 (2) | 340 (2) | 954 (2) | 27 |
| Mn(2)A | 1987 (2) | 592 (2) | 608 (2) | 26 |
| Mn(3)A | 2448 (2) | 1110 (2) | 2170 (2) | 28 |
| Mn(4)A | 2858 (2) | 9212 (2) | 1821 (2) | 30 |
| Mn(5)A | 2763 (2) | 1626 (2) | 9834 (2) | 27 |
| Mn(6)A | 2331 (2) | 9922 (2) | 9279 (2) | 29 |
| O(7)A | 2619 (6) | 311 (7) | 1427 (7) | 21 (4) |
| O(8)A | 2564 (6) | 618 (7) | 117 (8) | 29 (4) |
| Mn(1)B | 6800 (1) | 4559 (2) | 4049 (2) | 24 |
| Mn(2)B | 8010 (2) | 4307 (2) | 4369 (2) | 24 |
| Mn(3)B | 7710 (2) | 3755 (2) | 5724 (2) | 29 |
| Mn(4)B | 7241 (2) | 5650 (2) | 5156 (2) | 29 |
| Mn(5)B | 7150 (2) | 3279 (2) | 3206 (2) | 27 |
| Mn(6)B | 7506 (2) | 5006 (2) | 2784 (2) | 28 |
| O(7)B | 7441 (6) | 4574 (7) | 4843 (8) | 28 (4) |
| O(8)B | 7373 (6) | 4256 (7) | 3573 (8) | 23 (3) |

[a] The A and B suffixes refer to the two independent molecules.

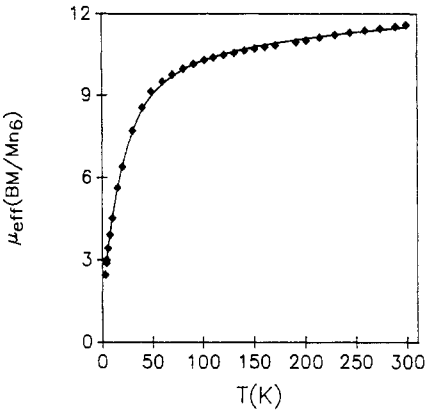


**Figure 3.** Plot of effective magnetic moment per $Mn_6$ complex, $\mu_{eff}/Mn_6$, versus temperature for $[Mn_6O_2(O_2CPh)_{10}(py)_2(MeCN)_2]\cdot 2H_2O$. The solid line results from a least-squares fit of the data to the theoretical susceptibility expression derived by the Kambe coupling method.

pathways connecting each of the $Mn^{III}$ ions, Mn(1) or Mn(2), to one pair of the $Mn^{II}$ ions, Mn(3,4) or Mn(5,6), are not equivalent. The appropriate bridging angles in the structure of **2** are noticeably different, e.g., Mn(1)–O(7)–Mn(3) and Mn(1)–O(7)–Mn(4) are 119.9 and 101.7°, respectively. A general spin–spin interaction model allowing for dissimilar coupling between the $Mn^{II}$–$Mn^{III}$ pairs could not be constructed by using the Kambe vector-coupling method[21b] for the isotropic Heisenberg spin Hamiltonian in eq 3, where $S_1 = S_2 = 2$ and $S_3 = S_4 = S_5$

$$H = -2JS_1\cdot S_2 - 2J_{2A}(S_1\cdot S_3 + S_2\cdot S_4 + S_1\cdot S_5 + S_2\cdot S_6) - 2J_{2B}(S_1\cdot S_4 + S_2\cdot S_3 + S_1\cdot S_6 + S_2\cdot S_5) - 2J_3(S_3\cdot S_4 + S_5\cdot S_6) \quad (3)$$

**Table IV.** Selected Bond Distances (Å) and Angles (deg) for **2**

(a) Bonds

| | | | | | | | |
|---|---|---|---|---|---|---|---|
| Mn(1)···Mn(2) | 2.820 (3) | Mn(2)···Mn(6) | 3.500 (3) | Mn(3)–O(7) | 2.184 (8) | Mn(4)–O(7) | 2.183 (8) |
| Mn(1)···Mn(3) | 3.532 (3) | Mn(3)···Mn(4) | 3.732 (3) | Mn(3)–O(11) | 2.122 (8) | Mn(4)–O(14) | 2.156 (8) |
| Mn(1)···Mn(4) | 3.167 (3) | Mn(5)···Mn(6) | 3.824 (3) | Mn(3)–O(23) | 2.149 (8) | Mn(4)–O(15) | 2.312 (8) |
| Mn(1)···Mn(5) | 3.543 (3) | Mn(3)···Mn(5) | 6.031 (3) | Mn(3)–O(30) | 2.327 (8) | Mn(4)–O(26) | 2.119 (8) |
| Mn(1)···Mn(6) | 3.139 (3) | Mn(3)···Mn(6) | 4.791 (3) | Mn(3)–O(33) | 2.131 (8) | Mn(4)–O(35) | 2.113 (8) |
| Mn(2)···Mn(3) | 3.177 (3) | Mn(4)···Mn(5) | 4.855 (3) | Mn(3)–N(39) | 2.294 (10) | Mn(4)–N(45) | 2.245 (11) |
| Mn(2)···Mn(4) | 3.507 (3) | Mn(4)···Mn(6) | 5.982 (3) | | | | |
| Mn(2)···Mn(5) | 3.159 (3) | | | Mn(5)–O(8) | 2.220 (8) | Mn(6)–O(8) | 2.198 (8) |
| | | | | Mn(5)–O(17) | 2.140 (8) | Mn(6)–O(9) | 2.263 (8) |
| Mn(1)–O(7) | 1.894 (8) | Mn(2)–O(7) | 1.895 (8) | Mn(5)–O(24) | 2.298 (8) | Mn(6)–O(20) | 2.158 (8) |
| Mn(1)–O(8) | 1.875 (8) | Mn(2)–O(8) | 1.884 (8) | Mn(5)–O(29) | 2.163 (8) | Mn(6)–O(32) | 2.112 (8) |
| Mn(1)–O(9) | 2.250 (8) | Mn(2)–O(21) | 1.957 (8) | Mn(5)–O(36) | 2.143 (8) | Mn(6)–O(38) | 2.121 (8) |
| Mn(1)–O(12) | 1.944 (8) | Mn(2)–O(24) | 2.227 (8) | Mn(5)–N(48) | 2.286 (10) | Mn(6)–N(54) | 2.279 (11) |
| Mn(1)–O(15) | 2.241 (8) | Mn(2)–O(27) | 1.945 (8) | | | | |
| Mn(1)–O(18) | 1.973 (8) | Mn(2)–O(30) | 2.234 (8) | | | | |

(b) Angles

| | | | | | | | |
|---|---|---|---|---|---|---|---|
| O(7)–Mn(1)–O(8) | 83.4 (3) | O(7)–Mn(2)–O(8) | 83.1 (3) | O(8)–Mn(5)–O(17) | 95.4 (3) | O(8)–Mn(6)–O(9) | 78.88 (28) |
| O(7)–Mn(1)–O(9) | 99.3 (3) | O(7)–Mn(2)–O(21) | 96.8 (3) | O(8)–Mn(5)–O(24) | 77.38 (27) | O(8)–Mn(6)–O(20) | 88.0 (3) |
| O(7)–Mn(1)–O(12) | 94.9 (3) | O(7)–Mn(2)–O(24) | 100.3 (3) | O(8)–Mn(5)–O(29) | 92.7 (3) | O(8)–Mn(6)–O(32) | 101.4 (3) |
| O(7)–Mn(1)–O(15) | 85.7 (3) | O(7)–Mn(2)–O(27) | 168.2 (3) | O(8)–Mn(5)–O(36) | 94.5 (3) | O(8)–Mn(6)–O(38) | 89.1 (3) |
| O(7)–Mn(1)–O(18) | 169.4 (3) | O(7)–Mn(2)–O(30) | 84.9 (3) | O(8)–Mn(5)–N(48) | 172.6 (3) | O(8)–Mn(6)–N(54) | 168.7 (3) |
| O(8)–Mn(1)–O(9) | 86.3 (3) | O(8)–Mn(2)–O(21) | 172.2 (3) | O(17)–Mn(5)–O(24) | 90.6 (3) | O(9)–Mn(6)–O(20) | 85.3 (3) |
| O(8)–Mn(1)–O(12) | 169.7 (3) | O(8)–Mn(2)–O(24) | 86.4 (3) | O(17)–Mn(5)–O(29) | 167.7 (3) | O(9)–Mn(6)–O(32) | 90.9 (3) |
| O(8)–Mn(1)–O(15) | 99.9 (3) | O(8)–Mn(2)–O(27) | 94.4 (3) | O(17)–Mn(5)–O(36) | 103.6 (3) | O(9)–Mn(6)–O(38) | 165.3 (3) |
| O(8)–Mn(1)–O(18) | 94.6 (3) | O(8)–Mn(2)–O(30) | 97.8 (3) | O(17)–Mn(5)–N(48) | 84.6 (3) | O(9)–Mn(6)–N(54) | 94.5 (3) |
| O(9)–Mn(1)–O(12) | 83.9 (3) | O(21)–Mn(2)–O(24) | 85.9 (3) | O(24)–Mn(5)–O(29) | 82.1 (3) | O(20)–Mn(6)–O(32) | 169.1 (3) |
| O(9)–Mn(1)–O(15) | 172.4 (3) | O(21)–Mn(2)–O(27) | 87.1 (3) | O(24)–Mn(5)–O(36) | 164.3 (3) | O(20)–Mn(6)–O(38) | 85.9 (3) |
| O(9)–Mn(1)–O(18) | 90.9 (3) | O(21)–Mn(2)–O(30) | 90.0 (3) | O(24)–Mn(5)–N(48) | 95.2 (3) | O(20)–Mn(6)–N(54) | 82.4 (3) |
| O(12)–Mn(1)–O(15) | 90.1 (3) | O(24)–Mn(2)–O(27) | 91.1 (3) | O(29)–Mn(5)–O(36) | 84.9 (3) | O(32)–Mn(6)–O(38) | 99.8 (3) |
| O(12)–Mn(1)–O(18) | 88.9 (3) | O(24)–Mn(2)–O(30) | 173.8 (3) | O(29)–Mn(5)–N(48) | 86.2 (3) | O(32)–Mn(6)–N(54) | 87.7 (3) |
| O(15)–Mn(1)–O(18) | 84.3 (3) | O(27)–Mn(2)–O(30) | 84.0 (3) | O(36)–Mn(5)–N(48) | 92.7 (3) | O(38)–Mn(6)–N(54) | 96.0 (3) |
| O(7)–Mn(3)–O(11) | 97.9 (3) | O(7)–Mn(4)–O(14) | 89.4 (3) | Mn(1)–O(7)–Mn(2) | 96.2 (3) | Mn(1)–O(8)–Mn(2) | 97.2 (3) |
| O(7)–Mn(3)–O(23) | 92.6 (3) | O(7)–Mn(4)–O(15) | 77.8 (3) | Mn(1)–O(7)–Mn(3) | 119.9 (4) | Mn(1)–O(8)–Mn(5) | 119.6 (4) |
| O(7)–Mn(3)–O(30) | 76.59 (27) | O(7)–Mn(4)–O(26) | 99.5 (3) | Mn(1)–O(7)–Mn(4) | 101.7 (3) | Mn(1)–O(8)–Mn(6) | 100.5 (3) |
| O(7)–Mn(3)–O(33) | 96.0 (3) | O(7)–Mn(4)–O(35) | 92.7 (3) | Mn(2)–O(7)–Mn(3) | 102.1 (3) | Mn(2)–O(8)–Mn(5) | 100.3 (3) |
| O(7)–Mn(3)–N(39) | 169.1 (3) | O(7)–Mn(4)–N(45) | 170.1 (3) | Mn(2)–O(7)–Mn(4) | 118.4 (4) | Mn(2)–O(8)–Mn(6) | 117.9 (4) |
| O(11)–Mn(3)–O(23) | 161.9 (3) | O(14)–Mn(4)–O(15) | 83.9 (3) | Mn(3)–O(7)–Mn(4) | 117.4 (3) | Mn(5)–O(8)–Mn(6) | 119.9 (3) |
| O(11)–Mn(3)–O(30) | 87.26 (28) | O(14)–Mn(4)–O(26) | 165.3 (3) | | | | |
| O(11)–Mn(3)–O(33) | 108.8 (3) | O(14)–Mn(4)–O(35) | 91.2 (3) | | | | |
| O(11)–Mn(3)–N(39) | 84.6 (3) | O(14)–Mn(4)–N(45) | 82.1 (3) | | | | |
| O(23)–Mn(3)–O(30) | 80.9 (3) | O(15)–Mn(4)–O(26) | 86.6 (3) | | | | |
| O(23)–Mn(3)–O(33) | 84.6 (3) | O(15)–Mn(4)–O(35) | 169.3 (3) | | | | |
| O(23)–Mn(3)–N(39) | 82.5 (3) | O(15)–Mn(4)–N(45) | 96.2 (3) | | | | |
| O(30)–Mn(3)–O(33) | 163.3 (3) | O(26)–Mn(4)–O(35) | 100.0 (3) | | | | |
| O(30)–Mn(3)–N(39) | 93.0 (3) | O(26)–Mn(4)–N(45) | 87.9 (3) | | | | |
| O(33)–Mn(3)–N(39) | 93.2 (3) | O(35)–Mn(4)–N(45) | 92.5 (4) | | | | |

**Table V.** Selected Bond Lengths (Å) and Angles (deg) for **3**[a]

| | | | |
|---|---|---|---|
| (a) Bonds | | | |
| Mn(1)···Mn(2) | 2.805 (6) | Mn(2)···Mn(6) | 3.131 (6) |
| Mn(1)···Mn(3) | 3.537 (6) | Mn(3)···Mn(4) | 3.839 (6) |
| Mn(1)···Mn(4) | 3.139 (6) | Mn(5)–Mn(6) | 3.798 (6) |
| Mn(1)···Mn(5) | 3.174 (6) | Mn(3)···Mn(5) | 4.890 (6) |
| Mn(1)···Mn(6) | 3.546 (6) | Mn(3)···Mn(6) | 6.011 (6) |
| Mn(2)···Mn(3) | 3.163 (6) | Mn(4)···Mn(5) | 6.053 (6) |
| Mn(2)···Mn(4) | 3.570 (6) | Mn(4)···Mn(6) | 4.850 (6) |
| Mn(2)···Mn(5) | 3.586 (6) | | |
| Mn(1)–O(7) | 1.884 (13) | Mn(2)–O(7) | 1.890 (14) |
| Mn(1)–O(8) | 1.913 (16) | Mn(2)–O(8) | 1.899 (15) |
| Mn(3)–O(7) | 2.203 (14) | Mn(4)–O(7) | 2.232 (14) |
| Mn(5)–O(8) | 2.240 (15) | Mn(6)–O(8) | 2.157 (15) |
| (b) Angles | | | |
| Mn(1)–O(7)–Mn(2) | 96.0 (6) | Mn(1)–O(8)–Mn(2) | 94.8 (7) |
| Mn(1)–O(7)–Mn(3) | 119.7 (6) | Mn(1)–O(8)–Mn(5) | 99.4 (6) |
| Mn(1)–O(7)–Mn(4) | 99.1 (6) | Mn(1)–O(8)–Mn(6) | 121.1 (7) |
| Mn(2)–O(7)–Mn(3) | 100.9 (6) | Mn(2)–O(8)–Mn(5) | 119.8 (7) |
| Mn(2)–O(7)–Mn(4) | 119.8 (7) | Mn(2)–O(8)–Mn(6) | 100.8 (6) |
| Mn(3)–O(7)–Mn(4) | 119.9 (6) | Mn(5)–O(8)–Mn(6) | 119.4 (7) |
| O(7)–Mn(1)–O(8) | 84.5 (6) | O(7)–Mn(2)–O(8) | 84.7 (6) |

[a] Data are for the $Mn_6O_2$ core of molecule A.

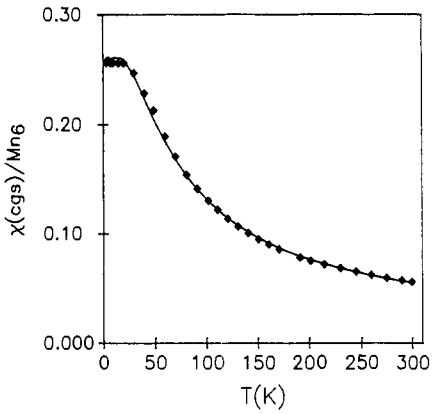


**Figure 4.** Plot of molar paramagnetic susceptibility, $\chi_M$, versus temperature for $[Mn_6O_2(O_2CPh)_{10}(py)_2(MeCN)_2]\cdot 2H_2O$. The solid line results from a least-squares fit of the data to the theoretical susceptibility expression derived by the Kambe coupling method.

$= S_6 = {}^5/_2$. To simplify the problem, the assumption was made that all of the $Mn^{II}$–$Mn^{III}$ exchange interactions ($J_{2A}$, $J_{2B}$) were equal to $J_2$, i.e., that the $Mn_6O_2$ core has the idealized symmetry ($D_{2h}$) of two edge-sharing tetrahedra. This allows the solution of the Hamiltonian matrix directly using the Kambe method.[21b] The following coupling scheme was chosen:

$$S_A = S_1 + S_2 \quad S_B = S_3 + S_4 \quad S_C = S_5 + S_6$$
$$S_D = S_B + S_C \quad S_T = S_A + S_D \tag{4}$$

The energies of the spin states in this coupling scheme are given in eq 5. The overall degeneracy of this spin system is 32 400,

$$E = -J_1[S_A(S_A + 1)] - J_2[S_T(S_T + 1) - S_A(S_A + 1) - S_D(S_D + 1)] - J_3[S_B(S_B + 1) + S_C(S_C + 1)] \tag{5}$$

which is made of 3176 different electronic states, with total spin values ranging from $S_T = 0$ to 14.

The molar paramagnetic susceptibility, $\chi_M$, was evaluated for this spin system by using the Van Vleck equation.[22] A computer subroutine was constructed that systematically characterized the 3176 spin states and derived the Van Vleck equation with its 3176 terms, and this was then incorporated into a nonlinear, least-squares computer program[16] that was used to fit the observed temperature dependence of $\mu_{eff}/Mn_6$ cluster as a function of the three exchange parameters, $J_1$, $J_2$, and $J_3$, and an isotropic $g$ value. Since the value of the parameter $g$ is best determined by the high-temperature data, only the data above 20 K were fit at first, and this gave $g = 1.90$, $J_1 = -38.2$ cm$^{-1}$, $J_2 = -1.0$ cm$^{-1}$, and $J_3 = -2.2$ cm$^{-1}$. During the fitting it was found that there was little correlation between the value of $g$ and the values of the three exchange parameters. However, an examination of the quality of this fit to the magnetic moment at the lowest temperatures (<10 K) showed a significant deviation between the calculated and observed curves. This discrepancy was also clearly evident in the calculated and experimental $\chi_M$ values where the calculated data passed through a maximum at <10 K and decreased rapidly while the experimental data leveled off and only slightly decreased in this region.

Possible reasons for this deviation include the neglect of single-ion zero-field splitting,[23] intercluster interactions,[24] a small percentage of paramagnetic impurity, or the assumption that $J_{2A} = J_{2B}$. In the case of contributions from single-ion zero-field splitting, it is not practical to include such contributions from the ions in the hexanuclear complex. The sequence of energy levels calculated from the values of exchange parameters for the above fit leads to an $S = 0$ ground state with a pair of degenerate $S_T = 1$ states and a set of degenerate $S_T = 2, 1, 0$ states at 4 and 9 cm$^{-1}$, respectively, above the ground state. The effect of single-ion zero-field splitting would be to cause a small splitting within each of these multiplets. This would not be expected to lead to a plateau in the susceptibility versus temperature profile. If the two $Mn^{II}$–$Mn^{III}$ interactions are not equal, the two $S_T = 1$ levels at 4 cm$^{-1}$ and other higher levels would no longer be degenerate. To test this possibility, calculations were made in which the two lowest $S_T = 1$ levels were systematically split symmetrically about their center of gravity in the higher symmetry model. In no case could the observed behavior be reproduced. Finally, the possibility that the low-temperature behavior of $\mu_{eff}/Mn_6$ is due to a small amount of paramagnetic impurity was examined. It was assumed that a small amount of a $Mn^{II}$, $S = {}^5/_2$, paramagnetic impurity was present, and the susceptibility data were fit to this model by using a least-squares-fitting computer program. A good fit was found with only 1.1% of a paramagnetic impurity. The nature of the impurity ion need only be one whose susceptibility obeys the Curie or Curie–Weiss law, and the most reasonable possibilities are mononuclear degradation products. The parameters for this fit are $g = 1.90$, $J_1 = -42.0$ cm$^{-1}$, $J_2 = -0.8$ cm$^{-1}$, and $J_3 = -2.4$ cm$^{-1}$. The calculated curves shown in Figures 3 and 4 agree well with the experimental data. The resulting order of the lowest lying spin states for this combination of parameters gives again an $S_T = 0$ ground state with two degenerate $S_T = 1$ states at 4 cm$^{-1}$ and degenerate $S_T = 0, 1, 2$ states at 9 cm$^{-1}$ at higher energy.

The values of the $Mn^{III}$–$Mn^{III}$, $Mn^{II}$–$Mn^{III}$, and $Mn^{II}$–$Mn^{II}$ exchange coupling parameters may be compared with those found recently for other polynuclear oxo-bridged manganese complexes, as listed in Table VI. The strongest interaction in complex **2** is between the two central bis($\mu$-oxide)-bridged $Mn^{III}$ ions ($J_1 = -42.0$ cm$^{-1}$). When compared with such interactions in the recently reported nonanuclear[11] and tetranuclear butterfly[9] complexes containing these same bridging units, this value appears quite reasonable. All three of these complexes contain two octahedrally coordinated $Mn^{III}$ ions sharing an edge comprised of two bis($\mu$-oxide) ions. The bond angles and bond lengths in these

(22) Van Vleck, J. H. *The Theory of Electric and Magnetic Susceptibilities*; Oxford University Press: London, 1932.
(23) Kennedy, B. J.; Murray, K. S. *Inorg. Chem.* **1985**, *24*, 1552.
(24) Ginsberg, A. P.; Lines, M. E. *Inorg. Chem.* **1972**, *11*, 2289.
(25) Diril, H.; Chang, H.-R.; Larsen, S. K.; Potenza, J. A.; Pierpont, C. G.; Schugar, H. J.; Isied, S. S.; Hendrickson, D. N. *J. Am. Chem. Soc.* **1987**, *109*, 6207.
(26) Bashkin, J. S.; Schake, A. R.; Vincent, J. B.; Chang, H.-R.; Huffman, J. C.; Christou, G.; Hendrickson, D. N. *J. Chem. Soc., Chem. Commun.* **1988**, 700.
(27) Chang, H.-R.; Larsen, S. K.; Boyd, P. D. W.; Pierpont, C. G.; Hendrickson, D. N. *J. Am. Chem. Soc.* **1988**, *110*, 4565.
(28) Vincent, J. B.; Li, Q.; Boyd, P. D. W.; Folting, K.; Huffman, J. C.; Hendrickson, D. N.; Christou, G. Submitted for publication.
(29) Sheats, J. E.; Czernuszewicz, R. S.; Dismukes, G. C.; Rheingold, A. L.; Petrouleas, V.; Stubbe, J.; Armstrong, W. H.; Beer, R. H.; Lippard, S. J. *J. Am. Chem. Soc.* **1987**, *109*, 1435.
(30) Koppen, M.; Fresen, G.; Wieghardt, K.; Llusen, R.; Nuber, B. *Inorg. Chem.* **1988**, *27*, 721.

**Table VI.** Exchange Parameters and $\mu$-Oxo Bridging Angles in Polynuclear Manganese Complexes[a]

| oxidn state | $J$, cm$^{-1}$ | bridging angle, deg | bond dist, Å |
|---|---|---|---|
| | Complex **2**[b] | | |
| II–II | −2.4 | 117.4, 119.9 | 2.183–2.220 |
| II–III | −0.8 | 88.1–119.6 | 1.874–2.220 |
| III–III | −42.0 | 96.2, 97.2 | 1.874–1.895 |
| | $Mn_9O_4(O_2CPh)_8(sal)_8(salH)_2(py)_4$[c] | | |
| II–III | −0.97 | 108.3–136.1 | 1.976–2.385 |
| III–III | −26.2 | 96.4, 96.9 | 1.878–1.896 |
| III–III | −11.2 | 129.4–133.1 | 1.872–1.896 |
| | $Mn_4O_2(O_2CMe)_6(bpy)_2$[d] | | |
| II–III | −1.97 | 112.4, 123.0 | 1.851–2.103 |
| III–III | −3.12 | 97.12 | 1.851, 1.856 |
| | $Mn_4O_2(O_2CMe)_7(bpy)_2^+$[d] | | |
| III–III | −7.80 | 123.2–131.3 | 1.844 |
| III–III | −23.53 | 95.7, 96.8 | 1.918, 1.911 |
| | $[Mn_2(bpmp)(O_2CMe)_2]^{2+}$[e] | | |
| II–III | −6.0 | 114.4 | 2.19, 1.90 |
| | $[Mn_2(bcmp)(O_2CMe)_2]^{2+}$[e] | | |
| II–III | −7.70 | 112.1 | 2.17, 1.96 |
| | $Mn_3O(O_2CMe)_6(py)_3\cdot py$[f] | | |
| II–III | −5.1 | 120.0 | 1.936 |
| III–III | −8.3 | 120.0 | 1.936 |
| | $Mn_2(bpy)_2(biphen)_2(biphenH)$[g] | | |
| II–III | +0.89 | 97.1, 102.4 | 2.142, 2.112 |
| | $[LMn_2Cl_2Br]\cdot H_2O$[h] | | |
| II–III | −1.7 | 102.5, 93.6 | 1.931–2.386 |
| | $[LMn_2Br_3]\cdot{}^1/_2CH_2Cl_2$[h] | | |
| II–III | −1.0 | | |
| | $Mn_2O(O_2CMe)_2(bpy)_2Cl_2$[i] | | |
| III–III | −4.1 | 124.3 | 1.777, 1.788 |
| | $Mn_2O(O_2CMe)_2(bpy)_2(N_3)_2$[i] | | |
| III–III | +3.4 | 122.0 | 1.802 |
| | $Mn_2O(O_2CMe)_2(HB(pz)_3)_2$[j] | | |
| III–III | −0.2 to −0.7 | 125.1 | 1.773 |
| | $[L'_2Mn_2O(O_2CMe)_2]^{2+}$[k] | | |
| III–III | +9 | 120.9 | 1.81 |

[a] Abbreviations: biphen$H_2$ = 2,2′-biphenol; $HB(pz)_3^-$ = hydrotris(1-pyrazolyl)borate; $LH_2$ = Schiff-base condensation product of 1,3-diaminopropane and 2,6-diformyl-4-*tert*-butylphenol; L′ = 1,4,7-trimethyl-1,4,7-triazacyclononane; bcmp is the same as bpmp (see ref 25) except that each of the bis(pyridylmethyl)amine units are replaced by 1,4,7-triazacyclononane units. [b] This work. [c] Reference 11. [d] Reference 9. [e] Reference 25. [f] Reference 12. [g] Reference 26. [h] Reference 27. [i] Reference 28. [j] Reference 29. [k] Reference 30.

units are all similar. The two longest bond lengths for each $Mn^{III}$ ion are trans oxygen atoms of bridging acetates, suggesting a Jahn–Teller elongation along these axes ($z$). The four unpaired electrons of each Mn atom in the $xz$, $yz$, $xy$, and $z^2$ orbitals are available for magnetic exchange interactions. In complex **2**, antiferromagnetic $\pi$ pathways are available between $xz$, $yz$ pairs via the bridging oxygen atom p orbitals, and antiferromagnetic $\sigma$ pathways between $xy$ pairs via oxygen s and p orbitals. The Mn $z^2$ electrons may interact via a ferromagnetic pathway involving an orthogonality at the bridging oxygen atom. The observed net antiferromagnetic interaction is as expected.

It is of interest to compare the $Mn^{III}$–$Mn^{III}$ exchange interactions in the present complex with those in mono($\mu$-oxide)-bridged $Mn^{III}$ complexes (Table VI). In all cases, the interactions in mono($\mu$-oxide)-bridged $Mn^{III}$ complexes are found to be smaller and, in some cases, ferromagnetic.[28,30]

In the case of the $Mn^{II}$–$Mn^{III}$ interactions, the value for the exchange parameter obtained for complex **2** is small and reflects an average of the exchange interactions for the two pathways with Mn–O–Mn bridging angles of ca. 100 and 120°. In the small collection of such molecules that have been examined, both ferromagnetic and antiferromagnetic interactions have been observed (Table VI). The bridging unit in **2** involves two distinct types of $\mu$-oxo bridges, namely the oxide ion and an oxygen atom of an acetate group. The Mn–O–Mn bridging angles of the acetate oxygen atoms are quite acute (ca. 88°).

The major exchange pathway connecting the $Mn^{II}$–$Mn^{III}$ pair through this carboxylate oxygen is via a $Mn^{III}$ $z^2$ orbital to a $Mn^{II}$ $x^2-y^2$ orbital, a $\sigma$ interaction. However, the small bridging angle for this pathway may lead to ferromagnetic coupling between these electrons as is found in many other $\mu$-oxo systems with small bridging M–O–M angles. The overall sign of the exchange parameter will reflect a combination of this and exchange interactions propagated via the oxide bridge, which has a larger Mn–O–Mn bridging angle. These latter interactions are found to be small and antiferromagnetic for bridging angles of 100–120° (Table VI).

**Concluding Comments.** The $Mn^{II}_4Mn^{III}_2$ complex **2** is not a very large complex relative to others that have been reported.[11,31] Nevertheless, complex **2** has 3176 low-lying electronic states as a result of magnetic exchange interactions between the constituent high-spin $Mn^{II}$ and $Mn^{III}$ ions. Even though complex **2** with its $S_T = 0$ ground state is not necessarily a good building block for preparing molecular ferromagnets, the synthetic strategies developed to prepare this $Mn^{II}_4Mn^{III}_2$ complex from a $Mn^{II}Mn^{III}_2$ reagent may prove useful in building even larger $Mn_x$ complexes.

Four different high-nuclearity Mn complexes have very recently been identified that do *not* have $S_T = 0$ ground states. First, we recently reported[32] the first $Mn^{III}_3Mn^{IV}$ complex, $(H_2Im)_2[Mn_4O_3Cl_6(HIm)(OAc)_3]\cdot{}^3/_2CH_3CN$ ($H_2Im^+$ = imidazolium cation). Detailed magnetization studies (1.8–40 K and 10–45 kG) have shown[34] that such complexes have a $S_T = {}^9/_2$ ground state with the lowest energy excited state more than 200 cm$^{-1}$ above it. Second, Caneschi et al.[33] reported the characterization of a $Mn^{II}_6$ complex where each $S = {}^5/_2$ $Mn^{II}$ ion has a nitronyl-nitroxide $S = {}^1/_2$ ligand. This aggregate has a $S_T = 12$ ground state, as indicated by magnetization versus magnetic field data obtained at 6 K with fields up to 2 kG. Third, we have reported[11] the X-ray structure and detailed modeling with a Kambe vector-coupling approach of the magnetic susceptibility data for the $Mn^{III}_8Mn^{II}$ complex $[Mn_9O_4(O_2CPh)_8(sal)_4(salH)_2(py)_4]$, which has a $S_T = {}^3/_2$ ground state. Finally, an analysis of detailed magnetization data collected at 10, 30, and 48 kG shows that the $Mn^{III}_8Mn^{IV}_4$ complex $[Mn_{12}O_{12}(O_2CPh)_{16}(H_2O)_4]$,[34] which has a structure similar to, but not identical with, the complex $[Mn_{12}O_{12}(O\text{-}Ac)_{16}(H_2O)_4]$ communicated by Lis,[31] has a $S_T = 14$ ground state.

The main lesson from these studies is that high-nuclearity $Mn_x$ complexes can be prepared which have either pairwise ferromagnetic $Mn^{II}$–$Mn^{II}$ or $Mn^{III}$–$Mn^{III}$ interactions or a combination of pairwise antiferromagnetic interactions that lead to molecules with $S_T \neq 0$ ground states. The $Mn_{12}$ complexes are being further examined to determine if there is any long-range ferromagnetic ordering in the solid state.

At least three strategies are available to try to prepare molecular ferromagnets from $Mn_x$ complexes. In one instance, high-nuclearity ferromagnetically coupled $Mn_x$ complexes can be prepared where there are weak magnetic exchange interactions between $Mn_x$ complexes in the solid state. Hydrogen-bonding and/or van der Waals interactions between $Mn_x$ complexes in the solid state may serve as the pathways for weak intermolecular, ferromagnetic interactions. The second strategy would be to prepare $Mn_x$ complexes that are large enough to function as ferromagnetically coupled, single-domain molecules, which could be magnetized. A third and perhaps more viable strategy would entail preparing

(31) Lis, T. *Acta Crystallogr., Sect. B.: Struct. Crystallogr. Cryst. Chem.* **1980**, *B36*, 2042.
(32) Bashkin, J. S.; Streib, W. E.; Huffman, J. C.; Chang, H.-R.; Hendrickson, D. N.; Christou, G. *J. Am. Chem. Soc.* **1987**, *109*, 6502.
(33) Caneschi, A.; Gatteschi, D.; Laugier, J.; Rey, P.; Sessoli, R.; Zanchini, C. *J. Am. Chem. Soc.* **1988**, *110*, 2795.
(34) Vincent, J. B.; Li, Q.; Boyd, P. D. W.; Folting, K.; Huffman, J. C.; Chang, H.-R.; Hendrickson, D. N.; Christou, G. *J. Am. Chem. Soc.* **1988**, *110*, 8537.

large $Mn_x$ complexes that exhibit intramolecular, ferromagnetic interactions and $S_T \neq 0$ ground states and then modify them so that there are bridges between two Mn ions, one from each of two neighboring $Mn_x$ complexes in the solid state. For example, there has been a recent report[35] of the preparation of polymeric forms of $[Fe_4S_4(SR)_4]^{2-}$ clusters that were prepared by employing difunctional thiolate ligands. If $Mn_x$ complexes with $S_T \neq 0$ ground states can be "cross-linked" in the solid state with ferromagnetic exchange propagating bridges, then long-range ferromagnetic ordering would be possible.

**Acknowledgment.** Funding from National Science Foundation Grant CHE-88-08019 (G.C.) and partial funding from National Institutes of Health Grant HL13652 (D.N.H.) are gratefully acknowledged. We thank the Bloomington Academic Computing Service for a gift of computer time.

**Registry No.** **1**, 109862-72-8; **2**, 120204-09-3; **3**, 120204-11-7; $(Et_3NH)_2[Mn(biphen)_2(biphenH)]$, 116275-78-6; $(Et_3NH)_2[Mn(Br_4biphen)_2(O_2CPh)]$, 120172-76-1; $Mn_6O_2(O_2CPh)_{10}(py)_2(MeCN)_2$, 120204-08-2.

**Supplementary Material Available:** Tables of fractional coordinates and thermal parameters, anisotropic thermal parameters of manganese ions, all bond lengths and angles for complexes **2** and **3**, and observed vs calculated susceptibility data and the distribution of spin states for **2** (32 pages); listings of calculated and observed structure factors for complexes **2** and **3** (32 pages). Ordering information is given on any current masthead page. Complete MSC structure reports for complexes **2** (No. 87 204) and **3** (No. 87 200) are available upon request from the Indiana University Chemistry Library.

(35) Ueyama, N.; Sugawara, T.; Nakamura, A.; Yamaguchi, K.; Fueno, T. *Chem. Lett.* **1988**, 223.

Contribution from the Department of Chemistry, Wake Forest University, Winston-Salem, North Carolina 27109, and Department of Radiology, Bowman Gray School of Medicine, Winston-Salem, North Carolina 27103

# Synthesis, Characterization, and Aqueous Proton Relaxation Enhancement of a Manganese(II) Heptaaza Macrocyclic Complex Having Pendant Arms

Bianke K. Wagnon[†] and Susan C. Jackels*[,†,‡]

*Received July 14, 1988*

The complex $Mn(NH_2Et)_2[15]pydieneN_5^{2+}$ has been prepared by template condensation of diacetylpyridine and penten in the presence of $Mn^{2+}$ in ethanol ($(NH_2Et)_2[15]pydieneN_5$ is 2,13-dimethyl-6,9-bis(2-aminoethyl)-3,6,9,12,18-pentaazabicyclo-[12.3.1]octadeca-1(18),2,12,14,16-pentaene and penten is *N,N,N′,N′*-tetrakis(2-aminoethyl)ethylenediamine). The complex is isolated as $Mn(NH_2Et)_2[15]pydieneN_5(PF_6)_2$ and can be converted to the $Cl^-$ salt for aqueous studies. The ligand is a 15-membered pentaaza macrocycle having two aminoethyl pendant arms that are branched from nitrogen atoms and that coordinate through amino groups at axial sites to give a pentagonal-bipyramidal complex. The high-spin Mn(II) complex has identical UV–visible spectra in aqueous and nonaqueous solvents. The EPR spectra are indicative of approximate axial symmetry. It is concluded that the aminoethyl groups are coordinated in solution as well as in the solid state. The aqueous proton NMR relaxation rate enhancement by the complex is 0.92 $mM^{-1}$ $s^{-1}$ at 24 MHz and 25 °C. In comparison to complexes with exchanging aquo coordination sites, the relaxation enhancement is small, indicative of relaxation via an outer-sphere mechanism only.

## Introduction

At present there is renewed interest in aqueous proton relaxation enhancement by paramagnetic metal complexes because of their application as contrast-enhancing agents for medical magnetic resonance imaging.[1] In particular, for a given complex, it is very desirable to be able to predict the aqueous proton relaxation enhancement over the frequency range of 0.01 to approximately 200 MHz. However, at present this is not possible because our quantitative understanding of relaxation enhancement extends only to the aquo ions. The lack of predictability for metal chelates arises from the fact that there are multiple contributions to the relaxation enhancement from the effects of inner-sphere water, outer-sphere water, and the field modulation of each through the fluctuations provided by molecular motions of solute and solvent and internal processes such as electron spin relaxation.[2] It is not possible to predict any of these components quantitatively, partially because very few complexes have been studied to date. One problem is the estimation of the fraction of the rate enhancement due to the solvating or outer-sphere water molecules. In this project the goal is to prepare a coordinatively saturated nonlabile complex having a ligand structure comparable to that of other known complexes. By comparison with analogous complexes having aquo ligands, the contributions of inner- and outer-sphere water can be estimated. To do this, we have prepared a macrocyclic complex of Mn(II) having coordinated pendant arms terminating in amine groups to ensure that the complex is coordinatively saturated by the ligand. Manganese(II) is preferred as the metal ion because it has good relaxation enhancement characteristics: long electron spin relaxation time and high magnetic moment. Related macrocyclic complexes of Mn(II) lacking the pendant arms and thus having inner-sphere water are available for comparison.

This paper describes the synthesis and characterization of the complex

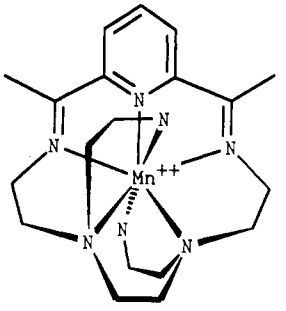


$Mn(NH_2Et)_2[15]pydieneN_5^{2+}$

The complex is based on the [15]pydieneN$_5$ macrocycle,[3] which is known to coordinate to Mn in an approximately pentagonal-planar fashion[4] but has in addition two aminoethyl pendant arms

* To whom correspondence should be addressed at Wake Forest University.
† Wake Forest University.
‡ Bowman Gray School of Medicine.

(1) Lauffer, R. B. *Chem. Rev.* **1987**, *87*, 901.
(2) Koenig, S. H.; Brown, R. D. III. In *Metal Ions in Biological Systems*; Sigel, H., Ed.; Marcel Dekker: New York, 1987; Vol. 21, Chapter 6.
(3) Alexander, M. D.; Van Heuvelen, A.; Hamilton, H. G., Jr. *Inorg. Nucl. Chem. Lett.* **1970**, *6*, 445.
(4) Van Heuvelen, A.; Lundeen, M. D.; Hamilton, H. G., Jr.; Alexander, M. D. *J. Chem. Phys.* **1969**, *50*, 489.

0020-1669/89/1328-1923$01.50/0 